Int. J. Electrochem. Sci., 8 **(2013)** 11860 - 11876

International Journal of
ELECTROCHEMICAL
SCIENCE
www.electrochemsci.org

Synthesis, Spectral Properties and Potentiometric Studies on Some Metal Schiff Base Complexes Derived from 4–chlorophenyl–2–aminothiazole

Abdel-Nasser M. A. Alaghaz[1*] *and Hoda A. Bayoumi*[2]

[1]Chemistry Department, Faculty of Science, Al–Azhar University, 11884, Nasr City, Cairo, Egypt.
[2]Chemistry Department, Girls College for Arts, Science and education, Ain Shams University, Cairo, P.O. BOX 11757, Egypt
[*]E-mail: aalajhaz@yahoo.com

Received: 7 July 2013 / *Accepted:* 1 August 2013 / *Published:* 15 September 2013

The complexes of type $[Cr(L)_2(H_2O)Cl]0.5H_2O$, $[Mn(L)_2(H_2O)_2]1.5H_2O$, $[Fe(L)_2(H_2O)Cl]2H_2O$, $[Co(L)_2(H_2O)_2]2H_2O$, $[Ni(L)_2(H_2O)_2]2H_2O$, $[Cu(L)_2.(H_2O)_2]2H_2O$, and $[Cd\text{-}(L)_2(H_2O)_2]1.5H_2O$, where L = salicylidene–4–chlorophenyl–2–aminothiazole, have been synthesized and characterized by different physical techniques. Protonation constants of Schiff base and stability constants of their binary metal complexes have been determined potentiometrically in 50% DMSO–water media at 25°C and ionic strength 0.10 M sodium perchlorate.

Keywords: Thiazole Schiff base; Transition metal complexes; Stability constants

1. INTRODUCTION

The condensation of primary amines with carbonyl compounds yields Schiff bases [1,2]. Schiff base with donors (N, O, S, etc) have structure similarities with neutral biological systems and due to presence of imine group are utilized in elucidating the mechanism of transformation of rasemination reaction in biological system [3]. Thiazole and its derivatives as ligands with potential sulphur and nitrogen bands are interesting and have gained special attention not only the structural chemistry of their multifunctional coordination modes but also of their importance in medicinal and pharmaceutical field. Schiff bases represent an important class of compounds because they are utilized as starting materials in the synthesis of industrial products [4].

The present study describes the coordination behaviour of novel Schiff base derived from the condensation of salicylaldehyde with 4–chlorophenyl–2–aminothiazole towards some transition elements, which may help in more understanding of the mode of chelation of HL towards metals. For

this purpose the complexes of Cr(III), Mn(II), Fe(III), Co(II), Ni(II) Cu(II) and Cd(II) ions with HL are studied in solution and in the solid state. The stability constants are evaluated and structure of the studied complexes is elucidated using elemental analyses, IR, MS, ^{1}H NMR, solid reflectance, magnetic moment, molar conductance, and thermal analyses measurements.

2. EXPERIMENTAL

2.1. Synthesis

2.1.1 Synthesis of the Salicylidene–4–chlorophenyl–2–aminothiazole (HL)

Hot solution (60 °C) of salicylaldehyde (3.03 g, 24.88 mmol) was mixed with hot solution (60 °C) of 4–chlorophenyl–2–aminothiazole (5.22 g, 24.88 mmol) in 50 mL ethanol. The resulting mixture was left under reflux for 2 h and the formed solid product was separated by filtration, purified by crystallization from ethanol, washed with diethyl ether and dried in a vacuum over anhydrous calcium chloride. The mixture was brought into reflux for 2 h. The orange product was produced in 93 % yield for HL.

2.1.2. Synthesis of the solid complexes

The metal complexes of the Schiff base HL was prepared by the addition of hot solution of the appropriate metal chloride (0.001 mmol) in methanol (8 mL) to the hot solution of the Schiff base (0.629 g HL, 0.002 mmol) in methanol (25 mL). The resulting mixture was stirred under reflux for 2 h where upon the complexes precipitated. They were collected by filtration and purified by washing with methanol and dried under vacuum over anhydrous $CaCl_2$.

2.2. Potentiometric titrations

Potentiometric measurements were made using a Metrohni 686 titroprocessor (Switzerland) equipped with a 665 Dosiniat. The electrode and titroprocessor were calibrated with standard buffer solutions prepared according to NBS specifications [5,6].

All Potentiometric measurements in this study were carried out in water–DMSO mixtures containing 50% DMSO because of low solubility of Schiff base and possible hydrolysis in aqueous solutions. The pk_w value in this medium was calculated to be 15.48.

2.2.1. Procedure of potentiometric measurements

Potentiometric titrations were carried out at constant temperature and an inert atmosphere of nitrogen with CO_2–free standardized 0.1M NaOH in 40 ml solution containing 0.1M $NaClO_4$:

(i) 3.0×10^{-3} M HNO_3 + 1.5×10^{-3} M Schiff base (for the protonation constant of the Schiff base);

(ii) 3.0×10^{-3} M HNO_3 +1.5 $\times10^{-3}$ M Schiff base + 7.5×10^{-4} M metal (II or III) ions (for the stability constant of the complexes). The species formed were characterized by the general equilibrium process (1), whereas the formation constants for these generalized species are given by Eq. (2) (charges are omitted for simplicity).

$$pM + qL + rH \rightleftharpoons M_pL_qH_r \quad (1)$$

$$\beta_{pqr} = \frac{[M_pL_qH_r]}{[M]^p[L]^q[H]^r} \quad (2)$$

Where M, L, H stand for the metal ion, ligand and proton, respectively. The calculations were performed using the computer program MINIQUAD–75 and were conducted on an IBM computer. The stoichiometries and stability constants of the complexes formed were determined by trying various possible composition models for the systems studied.

2.3. Physical measurements

All melting points were taken on a Stuart apparatus and are uncorrected. Elemental microanalyses of the solid chelates for C, H, N, S and Cl were performed at the Microanalytical Center, Cairo University. Metal contents were estimated on an AA–640–13 Shimadzu flame atomic absorption spectrophotometer in solution prepared by decomposing the respective complex in hot concentrated HNO_3. The molar conductance of solid chelates in DMF was measured using Sybron–Barnstead conductometer (Meter–PM.6, E = 3406). Their IR spectra were recorded on Perkin–Elmer FT–IR spectrophotometer in nujol mull and polyethylene pellets. The UV–visible absorption spectra were recorded using Jasco V–350 recording spectrophotometer at room temperature. The magnetic susceptibility was measured on powdered samples using the Faraday method. The diamagnetic corrections were made by Pascal's constant and $Hg[Co(SCN)_4]$ was used as a calibrant. The mass spectra were recorded by the EI technique at 70 eV using MS–5988 GC–MS Hewlett–Packard instrument in the Microanalytical Center, Cairo University. The ^1H NMR spectra were recorded using 300 MHz Varian–Oxford Mercury. The deuterated solvent used was dimethylsulphoxide (DMSO) and the spectra extended from 0 to 15 ppm. Rigaku model 8150 thermoanalyser (Thermaflex) was used for simultaneous recording of TG–DTA curves at a heating rate of 5° C min^{-1}. For TG, the instrument was calibrated using calcium oxalate while for DTA, calibration was done using indium metal, both of which were supplied along with the instrument in ambient condition. A flat bed type aluminium crucible was used with α-alumina (99% pure) as the reference material for DTA. The number of decomposition steps was identified using TG.

3. RESULTS AND DISCUSSION

3.1. Characterization of Schiff base

The ligand (Figure 1) was found to be soluble in $CHCl_3$, EtOH, MeOH, DMF, DMSO, THF, and insoluble in diethyl ether and water, slightly soluble in benzene and *n*-hexane. The structure of the

ligand (HL) was elucidated by elemental analyses, IR, electronic, ^{1}H NMR techniques. The assignment of the proposed structure for HL is based on the elemental analyses data listed in Table 1. The ligand may show keto–enol (Figure 1) tautomerism because it contains the amide bonds.

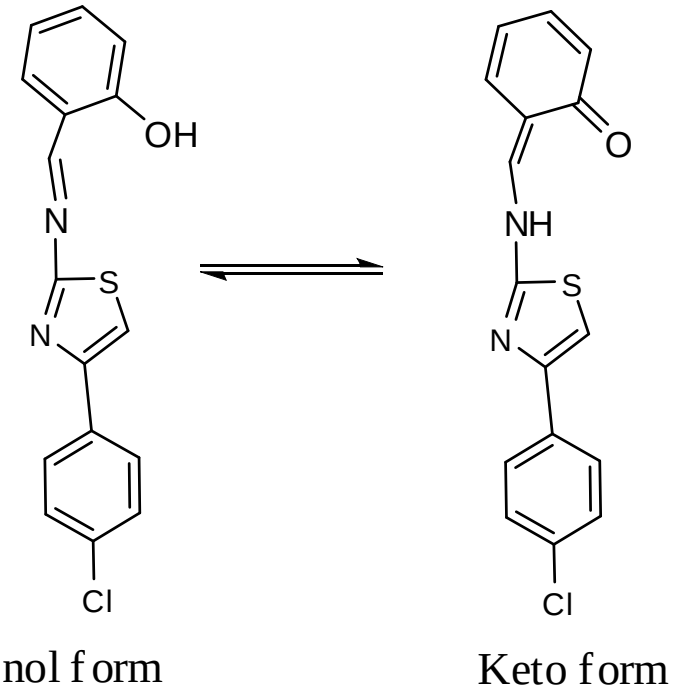

Figure 1. Proposed structure of the ligand (HL).

Table 1. Physical data of Ligand (HL) and corresponding metal complexes

Compound no. M. F. [M.Wt.]	m.p. (°C)	Color [Yield (%)]	Elemental analyses % calculated (found)						$^a\Lambda_m$
			M	C	H	N	S	Cl	
[HL] $C_{16}H_{11}ClN_2OS$ [314.79]	160	Orange [98]	--	61.05 (61.05)	3.52 (3.44)	8.90 (8.25)	10.19 (10.19)	11.26 (11.26)	--
(1)[$Cr(L)_2(H_2O)Cl$]0.5H_2O $C_{32}H_{23}Cl_3CrN_4O_{3.5}S_2$[742.03]	>300	Gray [89]	7.01 (7.00)	51.80 (51.05)	3.12 (3.11)	7.55 (7.45)	8.64 (8.54)	14.33 (14.27)	20.20
(2)[$Mn(L)_2(H_2O)_2$]1.5H_2O C C $_{32}H_{27}Cl_2MnN_4O_{5.5}S_2$ [745.55]	>300	Rose [90]	7.37 (7.36)	51.55 (51.53)	3.65 (3.64)	7.51 (7.50)	8.60 (8.58)	9.51 (9.46)	17.33
(3)[$Fe(L)_2(H_2O)Cl$]2H_2O $C_{32}H_{26}Cl_3FeN_4O_5S_2$ [772.91]	>300	Pale yellow [88]	7.23 (7.22)	49.73 (49.73)	3.39 (3.32)	7.25 (7.23)	8.30 (8.28)	13.76 (13.64)	18.05
(4)[$Co(L)_2(H_2O)_2$]2H_2O $C_{32}H_{28}Cl_2CoN_4O_6S_2$ [757.02]	>300	Green [91]	7.77 (7.73)	75 50.67 (50.63)	3.72 (3.70)	7.39 (7.32)	8.45 (8.43)	9.35 (9.33)	16.53
(5)[$Ni(L)_2(H_2O)_2$]2H_2O $C_{32}H_{28}Cl_2N_4NiO_6S_2$ [653.4]	>300	Dark green [90]	7.74 (7.73)	50.68 (50.66)	3.72 (3.71)	7.39 (7.34)	8.46 (8.45)	9.35 (9.34)	15.55
(6)[$Cu(L)_2(H_2O)_2$]2H_2O $C_{32}H_{28}Cl_2CuN_4O_6S_2$ [763.17]	>300	Dark brown [84]	8.33 (8.32)	50.36 (50.35)	3.70 (3.70)	7.34 (7.33)	8.40 (8.38)	9.29 (9.22)	10.12
(7)[$Cd(L)_2(H_2O)_2$]H_2O $C_{32}H_{26}Cl_2N_4O_5S_2Cd$ [794.02]	>300	Orange [88]	14.16 (14.14)	48.40 (48.38)	3.30 (3.29)	7.06 (7.00)	8.08 (8.07)	8.93 (8.92)	10.25

Table 2. Characteristic IR bands of the ligand and its metal complexes

Assignments	Ligand (HL)	1	2	3	4	5	6	7
ν(NH)	3272 br	–	–	–	–	–	–	–
ν(OH)	3545 br	–	–	–	–	–	–	–
ν(C–O)	1212m	1208m	1208m	1209m	1208m	1207m	1209m	**1206m**
ν(C=N)$_{azomethine}$	1641m	1614m	1614m	1616m	1616m	1615m	1614m	**1612m**
ν(C=N)$_{thiazole}$	1688m	1687m	1687m	1687m	1688m	1689m	1689m	**1690m**
ν(C–H)$_{aromatic}$	3034m	3033m	3033m	3032m	3034m	3034m	3032m	**3032m**
ν(C=C)$_{phenyl}$	1367m	1367m	1336m	1337 s	1335m	1334 s	1335m	**1334 s**
ν(C–S–C)$_{thiazole}$	744s	742s	742s	742s	743s	741s	742s	**743s**
ρr(H_2O)	-	838m	837m	745s	744s	788s	837s	**807s**
ρw(H_2O)	-	633m	615m	614s	625s	633s	624s	**630s**
δ(O–M−O)	-	187w	188 w	187 w	188 w	193 w	192 w	**193 w**
δ(O–M–N)	-	216w	218w	217 w	216 w	233 w	232 w	**233 w**
ν(M–$N_{Schiff\ base}$)	-	275m	270m	278m	290m	292m	290m	**294m**
ν(M–O)	-	335m	333m	333m	332m	342m	333m	**340m**
ν(M–$Cl_{terminal}$	-	**320m**	**322m**	**322m**	**324m**	**325m**	**320m**	**328m**

Where br = broad, s = strong, m = medium, w = weak, v.w = very weak

The IR spectrum (Table 2) does not show a ν(OH) band at 3545 cm^{-1} but shows the band at 3272 cm^{-1} corresponding to ν(NH), indicating that in solid state, the ligand exists in the keto form [7]. However, the ^1H NMR spectrum of ligand exhibits a sharp singlet at 11.88 ppm due to enolic –OH which indicates that the amide groups are transformed into iminol groups in solution [8]. The electronic spectrum of HL in ethanol showed absorption bands at 240–390 nm regions which is due to intraligand π→π* and n→π* transitions involving molecular orbital of the thiazole ring, a broad shoulder at approximately 435 nm were observed. The latter band is attributed to a n(oxygen) →π* transition of the dipolar zwitterionic structure or keto–amine tautomer of HL [7]. The electron impact mass spectrum (Figure 2) of the free ligand, confirms the proposed formula by showing a peak at 314 u corresponding to the ligand moiety [($C_{16}H_{11}ClN_2OS$) atomic mass 314.79u]. The series of peaks in the range, i.e. 66, 85, 94, 108, 134, 150 and 165 u, etc., may be assigned to various fragments and their intensity gives an idea of stability of fragments. The mass spectrum of the ligand (HL) shows the fragmentation pattern in Figure 3.

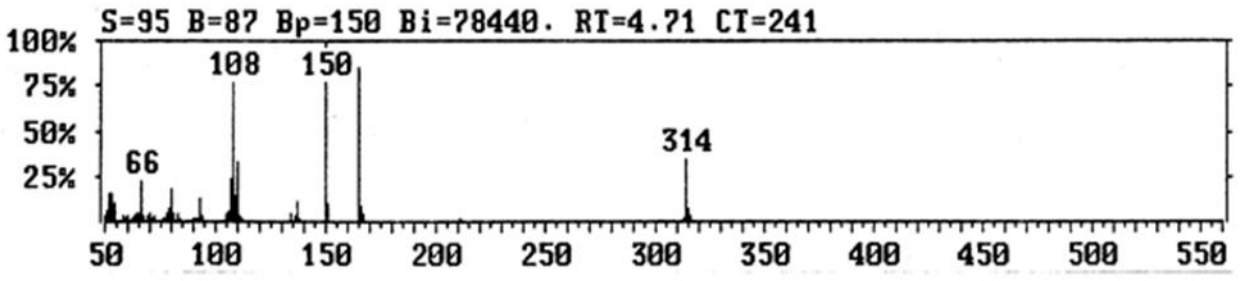

Figure 2. Mass spectrum of the ligand (HL).

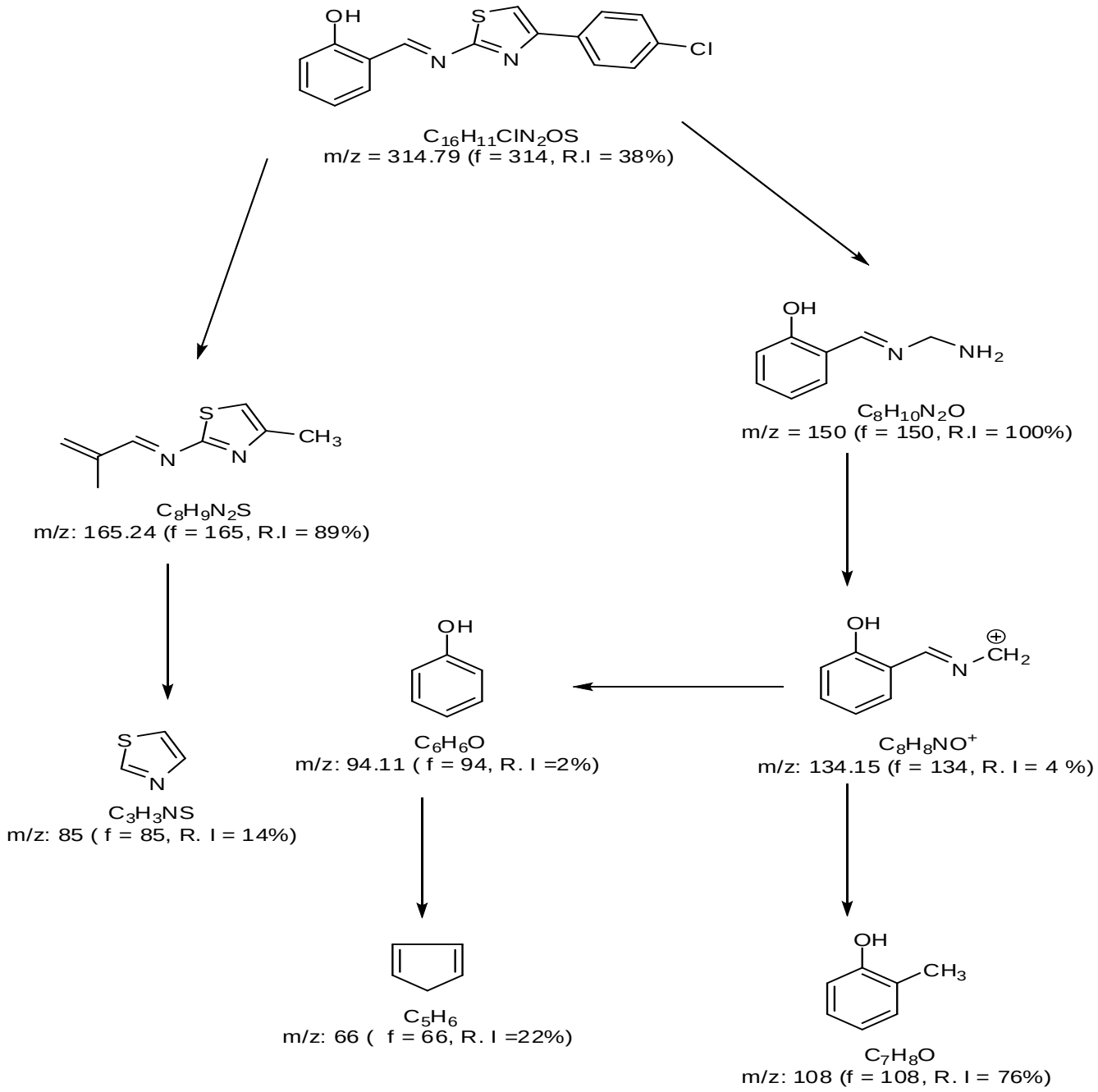

Figure 3. Fragmentation of the mass spectrum of the HL ligand.

3.2. Molar conductance measurements

The results given in Table 1 show that the Cr(III), Mn(II), Fe(III), Co(II), Ni(II), Cu(II) and Cd(II) complexes have a molar conductivity values in the range 7.12–10.20 Ω^{-1} mol^{-1} cm^2, which indicates the non–ionic nature of these complexes and they are considered as non-electrolyte [7]. This can be accounted for by the satisfaction of the bi– or tri–valency of the metal by the chloride. This implies the coordination of the anions to the metal ion centers.

3.3. Potentiometric studies

3.3.1. Protonation constants of Schiff base ligand (HL)

The study of complex formation by the studied Schiff base cannot be carried out in aqueous solution because of the nature of the compounds involved. These metal complexes as well as the ligand themselves are insoluble in water.

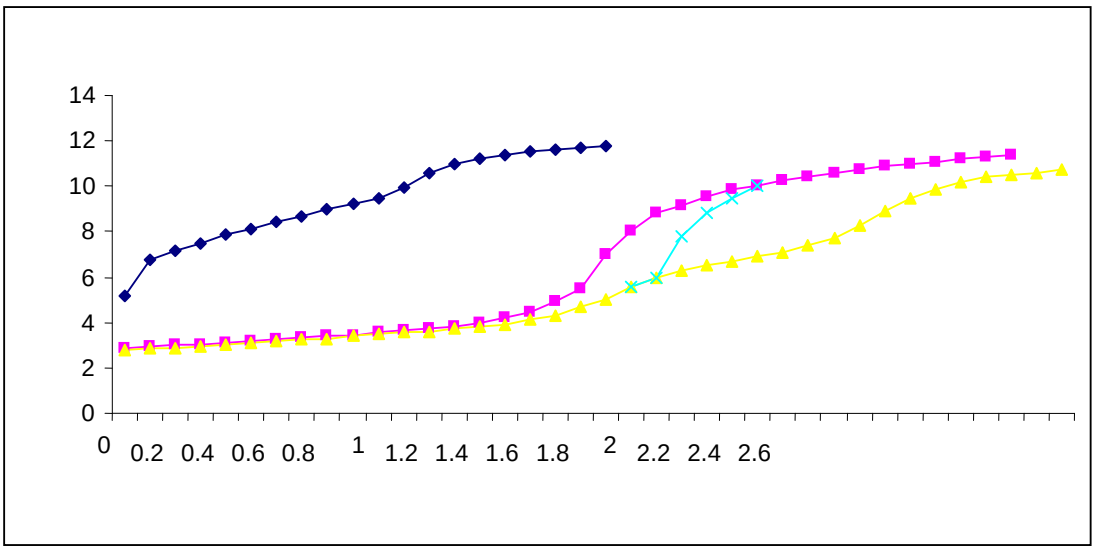

Figure 4. Potentiometric titration curve of the Cu(II)-L system.

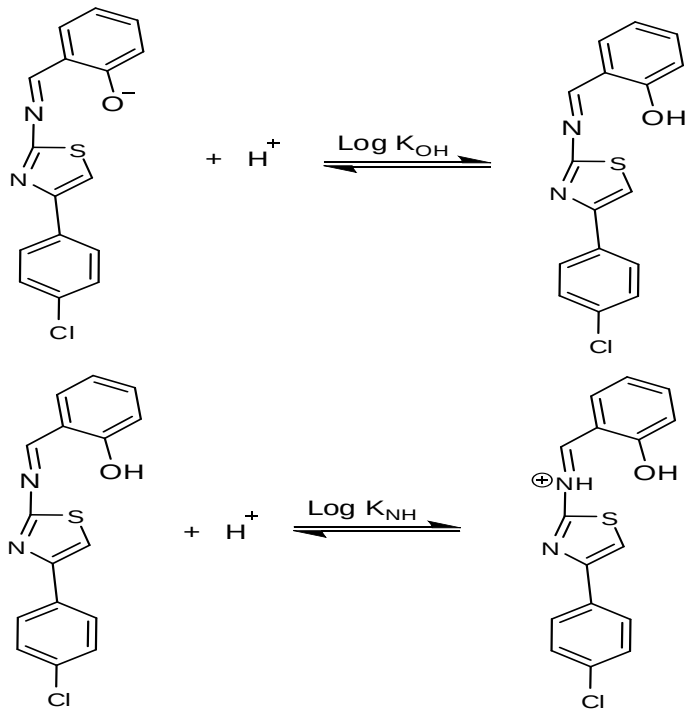

Figure 5. The log K_{OH} and log K_{NH} equilibrium reactions of the ligand HL.

This solvent has been most widely used for potentiometric determination of stability constants. The mixture DMSO–water 50: 50 % was the chosen solvent for our study. In such a medium, the studied Schiff base and their metal complexes are soluble giving stable solutions. The use of this mixed solvent has some advantages over pure DMSO. Thus, pure DMSO is very hygroscopic and controlling its water content is difficult [9]. This fact would affect reproducibility of our experiments. However, DMSO–water 50:50 % mixture has only a small hygroscopic character.

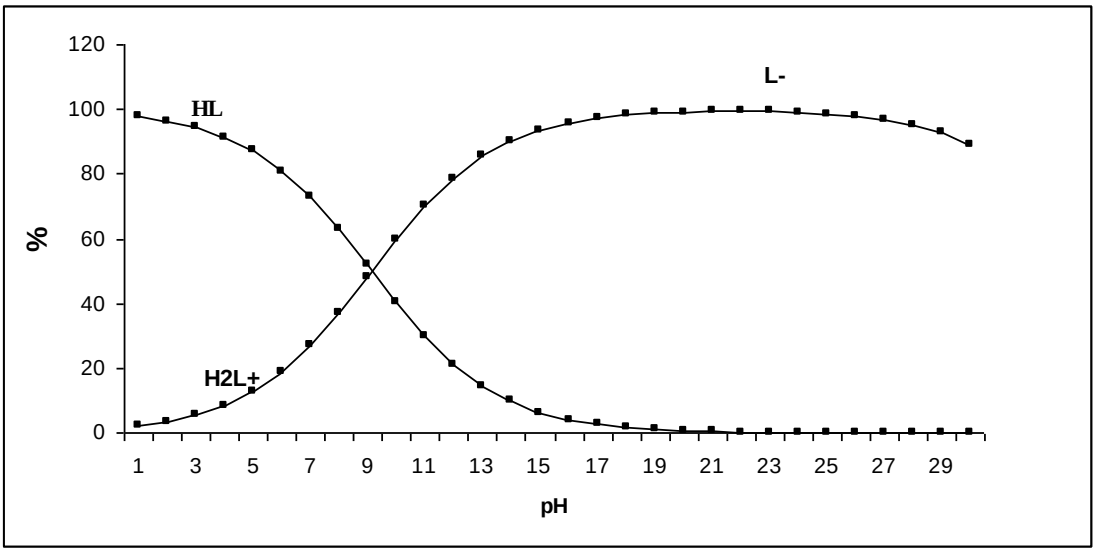

Figure 6. Species distribution diagram for the systems L Schiff base (HL) as a function of pH.

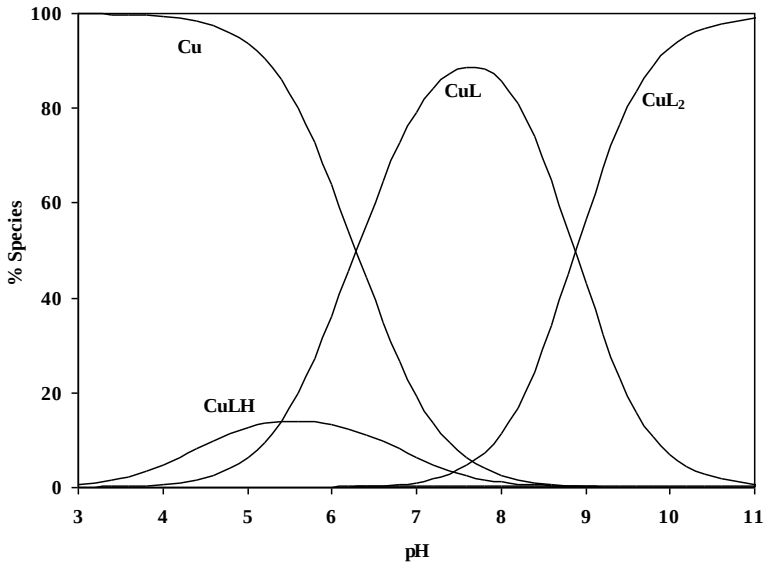

Figure 7. Species distribution diagram for the systems Cu(II)-Schiff base (HL) as a function of pH.

The stoichiometric protonation constants of the investigated Schiff base HL was determined in 50% DMSO–water at 25°C and these constants are tabulated in Table 3. As the titration curve of the

ligand in Figure 4, it can be seen that there are two end–points at a = 1 and a = 2. According to the results obtained from this titration curve it can be concluded that the Schiff base have two protonation constants. Log K_{OH} and Log K_{NH} values are amounting to 8.67 and 2.78 respectively, as Figure 5. The highest values due to the protonation of phenolic oxygen while the other value due to the imine nitrogen proton. The concentration distribution diagram of the protonated forms of the ligand are shown in Figure 6.

3.3.2. Stability constants of the Schiff base complexes

The potentiometric titration curves of the Cu(II)–L system, taken as a representative, are given in Figure 4. The titration curve of the Cu(II)–L complex is lowered from that of the free Schiff base(HL) curve, indicating formation of Cu(II) complex by displacement of protons. The formation constants were determined by fitting potentiometric data on the basis of possible composition models.

Table 3. The stability constants of of the metal complexes.

System	p	Q	r[a]	Log β [b]	S[c]
Ligand	0	1	1	8.67(0.01)	**3.8× 10^{-9}**
	0	1	2	11.45(0.02)	
Cu(II)	1	1	0	4.97(0.01)	**6.3× 10^{-9}**
	1	2	0	10.12(0.03)	
	1	1	1	15.23(0.03)	
Cr(III)	1	1	0	4.72(0.02)	**2.1× 10^{-8}**
	1	2	0	9.34(0.02)	
	1	1	1	14.66(0.01)	
Co(II)	1	1	0	3.57(0.04)	**9.3× 10^{-7}**
	1	2	0	7.63(0.06)	
	1	1	1	15.56(0.02)	
Ni(II)	1	1	0	3.11(0.03)	**7.0× 10^{-8}**
	1	2	0	6.33(0.05)	
	1	1	1	15.74(0.02)	
Cd(II)	**1**	**1**	**0**	**3.06(0.01)**	**9.9× 10^{-8}**
	1	**2**	**0**	**6.15(0.06)**	
	1	**1**	**1**	**14.24(0.02)**	

[a]*p, q* and *r* are the stoichiometric coefficients corresponding to metal ion, ligand and H^+, respectively; [b]Standar deviations are given in parentheses; [c]Sum of square of residuals .

The selected model with the best statistical fit was found to consist of CuL_2H_2, CuL_2H and CuL_2 complexes. The stability constants of their complexes are given in Table 3. The concentration distribution for the Cu(II) complex, taken as a representative, is given in Figure 7. The CuL complex starts to form at pH value 4, reaching a maximum concentration (88.61%). On the other hand, CuL_2 complex concentration was found to increase with increasing the pH and becomes predominant (95.14%) at pH=10.2. Protonated complex (CuHL) species have been found to be most favored at lower pH values.

The results show that the stability of the metal chelates follows the order Co<Ni<Cr<Cu>Cd. This order is in good agreement with that found by Mellor and Maley [10] and by Irving and Williams [11] for 3d transition metal ions. The classic sharp maximum for the Cu(II) complex is due to the stabilizing contribution of the Jahn–Teller effect With respect to increasing electronegativity of the metals, the electronegativity difference between metal atom and donor atom of the ligand will decrease, hence the metal–ligand bond would have more covalent character which may result in greater stability of the metal chelates [12].

3.4. Infrared spectra of the free ligands and their metal complexes

The IR spectra of Schiff base ligand (HL) and its complexes were carried out in the range 4000–400 cm^{-1} and 400–100 cm^{-1} (Table 2). The IR spectra of the complexes are compared with those of the free ligand in order to determine the coordination sites that may be involved in chelation. There are some guide peaks, in the spectra of the ligand, which are of good help for achieving this goal. The position and/or the intensities of these peaks are expected to be changed upon chelation. Upon comparison it is found that:

(1) The IR spectrum of the ligand shows a broad band at 3545 cm^{-1}, which can be attributed to phenolic OH group. This band disappears in all complexes, which can be attributed to the involvement of phenolic OH in coordination. The involvement of deprotonated phenolic moiety in complexes is confirmed by the shift of ν(C–O) stretching band observed at 1212 cm^{-1} in the free ligand to a lower frequency to the extent of 10–20 cm^{-1} [7]. The shift of ν(C–O) band at 1212 cm^{-1} to a lower frequency suggests the weakening of ν(C–O) and formation of stronger M–O bond.

(2) The medium bands observed in the 1641–1612 cm^{-1} frequency ranges in complexes were assigned to ν(C=N) mode. The shift of ν(C=N) vibration in all the complexes to a lower frequency suggests that the nitrogen atom of the ring contributes to the complexation. The lower ν(C=N) frequency indicates stronger M–N bonding [7].

(3) The medium and low intensity bands due to ν(C–S) and ν(C=N) modes of thiazole ring in the 1687–1690 and 741–744 cm^{-1} frequency ranges shifted to the lower frequency region (3136–3188 cm^{-1}) which suggests the weakening of C–S and C=N bonds and formation of M–S and M–S bonds [13].

(4) In the IR spectra of the complexes, a bands are observed at 270– 494 and 320 – 328 cm^{-1} that is attributed to the $\nu(M–N_{Schiff\ base})$ [14] and $\nu(M–Cl_{terminal})$ [15] stretching vibrations, respectively. Another band appeared between 332 and 342 cm^{-1}, which is assigned to the interaction of phenolic oxygen to the metal atom, i.e., the stretching vibrations ν(M–O) [14].

(5) Also, in the IR spectra of the complexes, a bands are observed at 187– 193 and 216 – 233 cm^{-1} that is attributed to the ν(O–M–O) and ν(O–M–N) [15] stretching vibrations, respectively.

(6) The bands in the range 744–837 cm^{-1} and 614–633 cm^{-1} appeared in the spectra of these complexes which may be assigned to $\rho r(H_2O)$ and $\rho w(H_2O)$ [7].

Therefore, from the IR spectra, it is concluded that HL behaves as a uninegative bidentate ligand with NO donor sites coordinating to the metal ions via the azomethine N and deprotonated phenolic–O atoms.

3.5. ^{1}H NMR spectra

The ^{1}H NMR spectra of Schiff base (HL) and its Cd(II) complex are recorded in d_6-dimethylsulfoxide (DMSO) solution using tetramethylsilane (TMS) as internal standard. The chemical shifts of the different types of protons for the ligand HL and its diamagnetic Cd(II) complex are listed in Table 4.

The spectrum of the complex is examined in comparison with those of the parent Schiff base. Upon examinations it is found that:

(1) The OH signal, appeared in the spectrum of HL ligand at 11.88 ppm (Table 4), completely [17] disappeared in the spectrum of its Cd(II) complex indicating that the OH proton is removed by the chelation with metal ion.

(2) The signal observed at 8.22 ppm for HL ligand is assigned to azomethine CH=N protons. This signal is found at 7.38 for Cd(II) complex. This indicates that the azomethine group (CH=N) is coordinated to the Cd(II) ion without proton displacement.

(3) The signal observed at 3.32 ppm with an integration corresponding to eight protons in case of Cd(II) complex is assigned to three water molecules.

We were unable to record the NMR spectra of the Cr(III), Mn(II), Fe(III), Co(II), Ni(II) and Cu(II) complexes due to their paramagnetic nature.

Therefore, it is clear from these results that the data obtained from the elemental analyses, IR and ^{1}H NMR spectral measurements are in agreement with each other.

Table 4. The ^{1}H NMR chemical shifts (ppm) for the Schiff base ligand HL, and its Cd(II) complex in DMSO solvent**.**

Compound	**^{1}H NMR**	
	Chemical shift, δ(ppm)	**Assignment**
HL	11.88*	**s, 2H, –OH**
	8.02*	**m, 2H, –NH**
	8.22*	**br, 1H, CH=N–**
$[Cd(L)_2(H_2O)_2]H_2O$	–	**2H, –OH**
	–	**m, 2H, –NH**
	7.38	**br, 2H, CH=N–**
	7.68–6.97	**Phenyl ring protons**
	3.32	**s, 6H, coordinated H_2O protons**

(1) s: singlet, br: broad, m: multiplet.

(2) Data given from the spectra depicted in Scheme 1.

(3) ^{1}H chemical Shifts were recorded in $CDCl_3$ solvent and referenced internally with respect to TMS.

(4) Asterisks (*) denote the bands disappeared after the addition of D_2O.

3.6. Electronic spectra and magnetic measurements

Electronic spectral data (Table 5) of the ligand (HL) was recorded in DMF solution. The electronic spectrum of ligand (HL) exhibited five absorption bands at 280, 312, 338, 422 and 433 nm. In this case, the first and third bands correspond to $^1L_a \leftarrow {}^1A_1$ and $^1L_b \leftarrow {}^1A_1$ transitions of the phenyl ring. The second band at 312 nm corresponds to the $\pi \rightarrow \pi^*$ transition of the C=O group. The fourth band at 422 nm corresponds to the $\pi \rightarrow \pi^*$ transition of the azomethine group, and the last band at 433 nm corresponds to the $n \rightarrow \pi^*$ due to the lone pairs of the oxygen and nitrogen.

The Cr(III) complex (1) $[Cr(L)_2(H_2O)Cl]0.5H_2O$ display bands at 556, 367, 367, and 265 nm, respectively. These bands may be assigned to $^4B_1g \rightarrow {}^4E_{1g}(\nu_1)$, $^4B_{1g} \rightarrow {}^4B_{2g}(\nu_2)$, $^4B_{1g} \rightarrow {}^4E_{1g}(\nu_3)$ and $^4B_{1g} \rightarrow {}^4A_{1g}(\nu_4)$ transitions, respectively, arising from the lifting of the degeneracy of the orbital triplet (in octahedral symmetry) in the order of increasing energy and assuming D_4h symmetry [19]. The C_4v symmetry has been ruled out because of higher splitting of the first band. This suggests it possess distorted octahedral geometry [19]. Chromium(III) complex shows magnetic moments corresponding to three unpaired electrons, i.e. 3.93 B.M., expected for high-spin octahedral chromium (III) complexes [19]. The electronic spectrum of the $[Mn(L)_2(H_2O)_2]1.5H_2O$ complex (2) shows a strong band at 768 nm which is assigned to the $^6A_{1g} \rightarrow {}^4T_{1g}$ (^4G) transition. The other characteristic bands for d–d transitions are difficult to recognize in this complex and thus the ligand field parameters could not be calculated [19]. The magnetic moment value is 5.46 B.M. which indicates the presence of Mn(II) complex in octahedral structure [20].

From the electronic spectrum it is observed that, the Fe(III) chelate (3) exhibits a band at 462 nm, which may be assigned to the $^6A_{1g} \rightarrow T_{2g}(G)$ transition in octahedral geometry of the complexes. The $^6A_{1g} \rightarrow {}^5T_{1g}$ transition appears to be split into two bands at 596 and 744 nm. The spectrum shows also a band at 368 nm which may be attributed to ligand to metal charge transfer [19]. The observed magnetic moment value of Fe(III) complex (3) $[Fe(L)_2(H_2O)Cl]2H_2O$ is found to be 5.56 B.M., indicating octahedral geometry around the Fe(III) complex (3) [21].

The electronic spectrum of the blue complex (4) $[Co(L)_2(H_2O)_2]2H_2O$ exhibits an intense band at 548 nm assignable to the $^4A_{2g}(F) \leftarrow {}^4T_{1g}(F)$ transition and a shoulder at 630 nm due to spin coupling, indicating octahedral geometry for this complex [19]. The blue color as well as the magnetic moment of 5.08 B.M is a further indication for the octahedral geometry [19].

The electronic spectrum of (5) $[Ni(L)_2(H_2O)_2]2H_2O$ is consistent with the octahedral geometry showing one broad d–d transition band at 789 nm assigned to $^3T_{1g}(F) \leftarrow {}^3A_{2g}(F)$ transition [19]. Magnetic moment of 2.87 B.M. is an additional evidence for the octahedral structure [19].

The electronic spectrum of the copper(II) complex (6) displays two strong bands at 292 and 397 nm which can be assigned to organic ligand → Cu and Cl → Cu charge transfer transitions [19-23], respectively. Furthermore, this spectrum consists of a broad d–d asymmetric band centred at about 715 nm (777 nm in DMSO solution). Presumably, all four d–d transitions ($^2A([\acute{\circ}d_{x^2-y^2}]^1) \rightarrow {}^2A([\acute{\circ}d_{z^2})^1]$, $^2A[(d_{xy})^1]$, $^2A[(dxz)^1]$, $^2A[(d_{yz})^1]$) of the octahedral geometry are responsible to this band.

The Cd(II) complex (7) $[Cd(L)_2(H_2O)_2]H_2O$ is diamagnetic and octahedral geometry is proposed for this complex.

Table 5. Molar conductance, magnetic moment and electronic spectral data of the ligand and its metal complexes

Complex	Geometry	μ_{eff} (B.M.)	Band assignments	λmax (nm)
[HL]	–	–	$^1L_a \leftarrow {}^1A_1$ $\pi \rightarrow \pi^*$ $^1L_b \leftarrow {}^1A_1$ $\pi \rightarrow \pi^*$ $n \rightarrow \pi^*$	**280** **312** **338** **422** **433**
(1)[Cr(L)$_2$(H$_2$O)Cl]0.5H$_2$O	Octahedral	3.93	$^4B_1g \rightarrow {}^4E_1g(\nu_1)$ $^4B_1g \rightarrow {}^4B_2g(\nu_2)$ $^4B_1g \rightarrow {}^4E_1g(\nu_3)$ $^4B_1g \rightarrow {}^4A_1g(\nu_4)$	**556** **367** **367** **265**
(2)[Mn (L)$_2$(H$_2$O)$_2$]1.5H$_2$O	Octahedral	5.46	$^6A_1g \rightarrow {}^4T_1g\ (^4G)$	**768**
(3)[Fe(L)$_2$(H$_2$O)Cl]2H$_2$O	Octahedral	5.56	$^6A_1g \rightarrow T_2g(G)$ $^6A_1g \rightarrow {}^5T_1g$ $^6A_1g \rightarrow {}^5T_1g$ LMCT (M←L)	**462** **596** **744** **368**
(4)[Co(L)$_2$(H$_2$O)$_2$]2H$_2$O	Octahedral	5.08	$^4T_1g \rightarrow {}^4T_2g(F)$ $^4T_1g \rightarrow {}^4A_2g(F)$	**630** **548**
(5)[Ni(L)$_2$(H$_2$O)$_2$]2H$_2$O	Octahedral	2.87	$^3A_2g(F) \rightarrow {}^3T_1g(F)$	**789**
(6)[Cu(L)$_2$(H$_2$O)$_2$]2H$_2$O	Octahedral	1.78	Ligand → Cu Cl → ligand ($^2A([\acute{\circ}d_{x^2-y^2})^1] \rightarrow {}^2A([\acute{\circ}d_{z^2})^1]$, $^2A[(d_{xy})^1]$, $^2A[(dxz)^1]$, $^2A[(d_{yz})^1]$)	**292** **397** **715**
(7)[Cd (L)$_2$(H$_2$O)$_2$]H$_2$O	**Octahedral**	**Diamagnetic**	**LMCT(M←N)**	**392**

3.7. Thermal analyses

Thermogravimetric (TG) and differential thermogravimetric (DTG) analysis were carried out for complexes 1, 2, 6 and 7, respectively. TGA results are in a good agreement with the suggested formulae resulted from microanalyses data (Table 1).

The Cr(III) complex (1) of HL is thermally decomposed in three stages; The first stage corresponds to a mass loss of 29.43 % (calcd. 29.44 %) within the temperature range 25–120°C represents the loss of half molecule of hydrated water, O_2, $4NH_3$, and 3HCl gases. The second stage corresponds to a mass loss of 2.41% (calcd. 2.42%) within the temperature range 120–270 °C represents the loss of one coordinated water. The third stage, 270–800 °C with a found mass loss of 43.24% (calcd. 43.26.89%), is reasonably accounted for the decomposition of the organic part of the complex leaving out $1/2Cr_2O_3$ as a residue with a found mass loss of 10.23% (calcd. 10.24%).

The Co(II) complex (4) of HL is thermally decomposed in three stages. The first stage corresponds to a mass loss of 4.74% (calcd. 4.75%) within the temperature range 25–125 °C represents the loss of two molecules of hydrated water. The second stage corresponds to a mass loss of 22.85% (calcd. 22.86%) within the temperature range 125–245 °C represents the loss of two coordinated water, O_2, $4NH_3$, and 2HCl gases. The third stage, 245–795 °C with a found mass loss of 52.63% (calcd. 52.63%), is reasonably accounted for the decomposition of the organic part of the complex leaving out CoO as a residue with a found mass loss of 19.75% (calcd. 19.76%).

The Cu(II) complex (6) of HL is thermally decomposed in three stages. The first stage corresponds to a mass loss of 4.69% (calcd. 4.72%) within the temperature range 30–130°C represents the loss of two molecules of hydrated water. The second stage corresponds to a mass loss of 24.22% (calcd. 24.24%) within the temperature range 130–255 °C represents the loss of two coordinated water, 2HCl, $1/2O_2$ and $4NH_3$ gases. The third stage, 255–790 °C with a found mass loss of 60.13% (calcd. 60.17%), is reasonably accounted for the decomposition of the organic part of the complex leaving out CuO as a residue with a found mass loss of 10.43% (calcd. 10.42%).

The Cd(II) complex (7) of HL is thermally decomposed in three stages. The first stage corresponds to a mass loss of 23.28% (calcd. 23.30%) within the temperature range 30–125°C represents the loss of two molecules of hydrated water, $4NH_3$, 2HCl and $1/2O_2$ gases. The second stage corresponds to a mass loss of 4.51% (calcd. 4.53%) within the temperature range 125–270 °C represents the loss of two coordinated water. The third stage, 270–800 °C with a found mass loss of 56.00% (calcd. 56.05%), is reasonably accounted for the decomposition of the organic part of the complex leaving out CdO as a residue with a found mass loss of 16.16% (calcd. 16.17%).

3.8. Kinetic studies

The thermodynamic activation parameters (Table 6–8) of decomposition processes of the metal complexes namely activation energy (E^*), entropy (ΔS^*) and Gibbs free energy change of the decomposition (ΔG^*) were evaluated graphically by employing three methods, Horowitz–Metzger [24] (HM), Coats–Redfern [25] (CR), and Piloyan–Novikova [26] (PN). From the results obtained, the following remarks can be pointed out:

Table 6. Kinetic parameters evaluated by Coats–Redfern equation

Compound	Stage	T(K)	A(S^{-1})	E_a (kJ/mol)	ΔH (kJ/mol)	ΔS (kJ/mol)	ΔG (kJ/mol)
(1)[Cr(L)$_2$(H_2O)Cl]0.5H_2O	1st	447	23.75×10^5	136.85	132.67	–0.053	**165**
	2nd	546	56.82×10^7	148.63	143.32	–0.077	**198**
(4)[Co(L) $_2$(H_2O)$_2$]2H_2O	1st	476	45.87×10^6	56.65	52.23	–0.097	**155**
	2nd	634	15.63×10^7	111.30	106.63	–0.110	**187**
(6)[Cu(L) $_2$(H_2O)$_2$]2H_2O	1st	487	86.88×10^7	112.21	109.64	–0.033	**154**
	2nd	589	11.23×10^7	144.33	140.67	–0.068	**187**
(7)[Cd (L) $_2$(H_2O)$_2$]H_2O	1st	465	3.07×10^9	43.65	55.15	−0.030	**167**
	2nd	**577**	**5.44×10^{11}**	**72.07**	**76.86**	**−0.072**	**186**

(1) The energy of activation (E) values increases on going from one decomposition stage to another for a given complex, indicating that the rate of decomposition decreases in the same order. Generally stepwise stability constants decreases with an increase in the number of ligand attached to a

metal ion. Conversely, during decomposition reaction the rate of removal of remaining ligands will be smaller after the expulsion of two ligands [27].

(2) The values of ΔG increases significantly for the subsequently decomposition stages due to increasing the values of (TΔS) from one stage to another. This may be attributed to the structural rigidity of the remaining complex after the expulsion of more ligands, as compared with the precedent complex, which require more energy, TΔS, for its rearrangement before undergoing any compositional change [27].

(3) The negative ΔS values for the decomposition steps indicate that all studied complexes are more ordered in their activated states, while the positive ΔH values mean that the decomposition processes are endothermic [27].

Table 7. Kinetic parameters evaluated by Horowitz–Metzger equation

Compound	Stage	T(K)	A(S^{-1})	E_a (kJ/mol)	ΔH (kJ/mol)	ΔS (kJ/mol)	ΔG (kJ/mol)
(1)[Cr(L)$_2$(H$_2$O)Cl]0.5H$_2$O	1st	447	22.32×10^5	138.24	130.76	–0.044	**163**
	2nd	546	53.78×10^7	148.12	142.89	–0.089	**187**
(4)[Co(L)$_2$(H$_2$O)$_2$]2H$_2$O	1st	476	44.44×10^6	58.42	51.78	–0.087	**156**
	2nd	634	16.14×10^7	112.22	103.78	–0.108	**194**
(6)[Cu(L)$_2$(H$_2$O)$_2$]2H$_2$O	1st	487	87.43×10^7	115.14	108.34	–0.046	**162**
	2nd	589	12.48×10^7	147.53	141.45	–0.073	**194**
(7)[Cd(L)$_2$(H$_2$O)$_2$]H$_2$O	1st	465	2.89×10^9	42.13	54.23	−0.030	**165**
	2nd	**577**	$\mathbf{4.99 \times 10^{11}}$	**70.26**	**72.87**	**−0.071**	**183**

Table 8. Kinetic parameters evaluated by Piloyan–Novikova equation

Compound	Stage	T(K)	A(S^{-1})	E_a (kJ/mol)	ΔH (kJ/mol)	ΔS (kJ/mol)	ΔG (kJ/mol)
(1)[Cr(L) $_2$(H$_2$O)Cl]0.5H$_2$O	1st	447	24.66×10^5	137.43	132.42	–0.064	**167**
	2nd	546	54.32×10^7	149.28	144.56	–0.073	**196**
(2)[Mn (L) $_2$(H$_2$O)$_2$]1.5H$_2$O	1st	476	44.68×10^6	55.78	53.64	–0.096	**153**
	2nd	634	17.39×10^7	114.76	105.45	–0.112	**184**
(3)[Fe(L)$_2$(H$_2$O)Cl]2H$_2$O	1st	487	84.63×10^7	114.57	110.12	–0.034	**152**
	2nd	589	13.21×10^7	143.45	143.56	–0.072	**184**
(7)[Cd(L)$_2$(H$_2$O)$_2$]H$_2$O	1st	465	3.04×10^9	40.44	52.46	−0.031	**163**
	2nd	**577**	$\mathbf{5.42 \times 10^{11}}$	**71.79**	**73.78**	**−0.070**	**184**

On the basis of the above observations and from the magnetic and solid reflectance measurements, octahedral geometry is suggested for the investigated complexes. The structure of the complexes is shown in Figure 8.

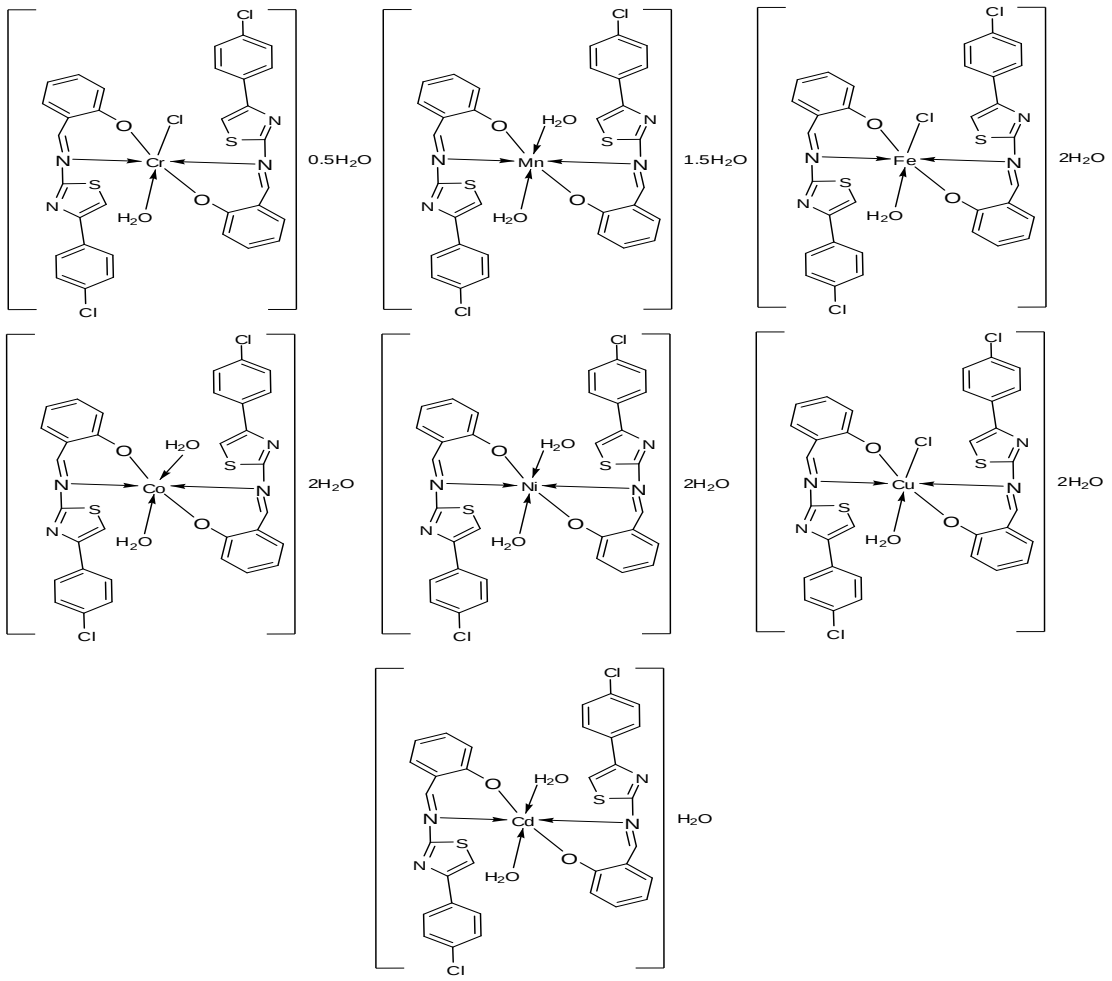

Figure 8. The proposed structures of HL complexes.

4. CONCLUSION

The straightforward condensation of *p*–chlorophenyl–2–aminothiazole and salicyaldehyde to yield the novel Schiff base ligand has been reported. Its flexible back bone, together with the presence of N and O donor atoms, renders this compound interesting for studying its coordination behaviour with transition metals ion. In this work some complexes with copper, nickel and cobalt have been characterized and all the data collected in agreement with the proposed structures. The spectral data indicate that ligand behaves as a neutral bidentate ligand, with two different coordinating sites, one provided by the hydroxyl group (OH) and one by the azomethine group (CH=N), each one accommodating a metal ion. Antimicrobial study reveals that, metal complexes have more biological activity than free ligand. Complexes (**1** and **3**) $[Cr(L)_2(H_2O)Cl]0.5H_2O$ and $[Fe(L)_2(H_2O)Cl]2H_2O$, respectively, shows best antimicrobial activity against all microorganism.

References

1. 1.Y. Shibuya, K. Nabari, M. Kondo,S. Yasue, K. Maedo, F. Uchida, H. Kawaguchi, *J. Chem. Lett.* 37 (2008) 78.

2. M. Bera, U. Mukhopadhyay, D. Ray, *Inorg. Chem. Acta* 358 (2008) 437.
3. L. A. Saghatforoush, F. Chalabian, A. Aminkhani,G. Karimnezhad, S. Ershad, *Eur. J. Med. Chem.* 44 (2009) 4490.
4. D.P. Singh, R. Kumar, J. Singh, *Eur. J. Med. Chem.* 44 (2009) 1731.
5. R.C. Bates, "*Determination of pH - Theory and Practice*" second ed., Wiley Interscience, New York, 1975.
6. H. Irving, H.S. Rossotti, *J. Chem. Soc.* 3397, 1953.
7. S. Chandra, A.K. Sharma, *Spectrochim. Acta A* 72 (2009) 851.
8. P.W. Alexander, R.J. Sleet, *Aust. J. Chem.* 23 (1970) 1183.
9. D. Martin, H.G. Hauthal, "*Dimethyl Sulphoxide*", Van Nostrand Reinhold, Wokingham, UK, 1975.
10. D.P. Mellor, L. Maley, *Nature* 159 (1947) 370.
11. H. Irving, R.J.P. Williams, *Analyst* 71 (1952) 813.
12. F.A. Cotton, G. Wilkinson, C.A. Murillo,M. Bochmann, "*Advanced Inorganic Chemistry*", sixth ed. Wiley, New York,1999.
13. A.M.A. Alaghaz, S.A.H. Elbohy, *Phosphorus, Sulfur, Silicon, Relat. Elem.* 183 (2008) 2000.
14. F.J. Barros–García, A. Bernalte–García, F.J. Higes–Rolando, F. Luna–Giles, A.M. Pizarro–Galán, E.Z. Viñuelas–Zahínos, *Anorg. Allg. Chem.* 631 (2005) 1898.
15. Y.J. Weaver, J.A.J. Weaver, *Nucl. Inorg. Chem.* 37 (1975) 1309.
16. B.K. Singh, U.K. Jetley, R.K. Sharma, B.S. Garg, *Spectrochim. Acta A* 63 (2006) 96.
17. A.B.P. Lever, "*Inorganic Electronic Spectroscopy*", second ed. Elsevier Science Publishers, Ch. 5, p. 203, 1984.
18. J. Gradinaru, A. Forni, V. Druta, S. Quici, A. Britchi, C. Deleanu, N. Gerbeleu, *Inorg. Chim. Acta* 338 (2002) 169.
19. F.A. Cotton, G. Wilkinson, "*Advanced Inorganic Chemistry, A Comprehensive Text*" fourth ed., John Wiley and Sons, New York, 1986.
20. B.J. Hathaway, G. Wilkinson, R.D. Gillard, J.A. McCleverty, (Eds.), "*Comprehensive Coordination Chemistry*", vol. 5,1987, Pergamon Press, Oxford.
21. R.L. Farmer, F.L. Urbach, *Inorg. Chem.* 13 (1974) 587.
22. M.F.R. Fouda, M.M. Abdel–Zaher, M.M.E. Shadofa, F.A. El Saied,M.I. Ayad, A.S. El–Tabl, *Trans. Met. Chem.* 33 (2008) 219.
23. N.N. Greenwood, T.C. Gibb, "*Mössbauer Spectroscopy*", 1st ed., Chapman and Hall Ltd. Publishers, London, p. 248, 1971.
24. H.H. Horowitz, G.J. Metzger, *Anal. Chem.* 1954 (1963).
25. A.W. Coats, J.P. Redfern, *Nature* 201 (1964) 68.
26. G.O. Piloyan, T.D. Pyabonikar, C.S. Novikova, *Nature* 212 (1966) 1229.
27. L.T. Valaev, G.G. Gospodinov, *Thermochim. Acta* 370 (2001) 15.